GeoVirtual 2020 September 14-16
Resilience and Innovation

Compressive resistance of helical piles subjected to seismic loads

Gustavo Padros
ARKK Engineering Corp., Sherwood Park, Alberta, Canada
Richard Schmidt
Almita Piling Inc., Edmonton, Alberta, Canada

ABSTRACT
Helical piles installed in seismic regions are subjected to the detrimental effects caused by dilatational and shear waves traveling through soils. The dilatational wave produces an increase in pore pressure, which leads to a decrease in the effective stress and consequently a decrease in the soil shear strength. Furthermore, shear wave propagation produces dynamic shear stresses, which are additive to the static shear stresses present in the soil mass prior to the earthquake. On this basis, seismic waves produce a decrease in soil resistance and an increase in shear stresses acting in the soil. A methodology based on Zeevaert's theory is presented in the present paper that allows designing helical piles for seismic loads, based on the determination of the increase in pore pressure due to dilatational waves and the increase in shear stresses due to shear waves.

RÉSUMÉ
Les pieux hélicoïdaux installés dans les régions sismiques sont soumis aux effets néfastes causés par les ondes de dilatation et de cisaillement traversant les sols. L'onde de dilatation produit une augmentation de la pression interstitielle, ce qui entraîne une diminution de la contrainte effective et par conséquent une diminution de la résistance au cisaillement du sol. De plus, la propagation des ondes de cisaillement produit des contraintes de cisaillement dynamiques, qui s'ajoutent aux contraintes de cisaillement statiques présentes dans la masse du sol avant le tremblement de terre. Sur cette base, les ondes sismiques produisent une diminution de la résistance du sol et une augmentation des contraintes de cisaillement agissant dans le sol. Une méthodologie basée sur la théorie de Zeevaert est présentée dans le présent article qui permet de concevoir des pieux hélicoïdaux pour les charges sismiques, sur la base de la détermination de l'augmentation de la pression interstitielle due aux ondes de dilatation et de l'augmentation des contraintes de cisaillement dues aux ondes de cisaillement.

1 INTRODUCTION

Helical piles may develop considerable compressive and uplift resistances, which make them viable as a deep foundation alternative in earthquake regions. The pile compressive resistance comprises shaft friction and end bearing, and if the helical pile has been manufactured with several helices installed relatively close (typically spaced apart not more than 3 times the helix diameter), a cylindrical shear resistance (CSR) is developed between the uppermost and lowermost helices, which also contributes to the compressive resistance of the pile. Furthermore, the uplift resistance of the helical pile comprises shaft friction and upward bearing of the uppermost helix. Piles manufactured with multiple helices adequately spaced also develop cylindrical shear resistance in uplift loading.

The determination of the compressive resistance of helical piles subjected to seismic loads requires assessing the effects that dilatational waves and shear waves produce in a saturated soil mass. Dilatational waves will cause an increment in pore water pressure, which will decrease the effective stress, thus reducing the end bearing resistance and cylindrical shear resistance (CSR) of the helical pile. Furthermore, shear waves propagating upwards will produce distortion of the soil layers, causing an increase in the soil shear stress, which will reduce the CSR available. In addition, the rocking of the superstructure will increase the pile loads. Therefore, the effects produced by dilatational waves and shear waves should be quantified and incorporated to the design of helical piles in earthquake regions. The surface (Rayleigh) wave is a third type of seismic wave, developed once the other waves reach the surface. The effects produced on foundations by surface waves are not considered herein.

Dilatational waves and shear waves are generated when the seismic waves produced by earthquakes reach the firm ground/soil deposits interphase. The dilatational

waves travel faster than the shear waves and are the first to arrive at the place of observation. The translation of dilatational waves requires changes in the soil volume. Therefore, dilatational waves develop high pore water pressures in saturated soils although they produce small displacements. On the contrary, shear waves do not produce volume changes in the soil during their propagation, but high shear distortions may be induced and shear stresses greater than the soil shear strength can be developed.

The objectives of the present paper are: (1) Present a methodology based on Zeevaert's theory (1980, 1982, 1988 and 1991) to determine the increase in pore water and the increase in the soil shear stress due to earthquakes; and (2) Apply the methodology to compute the compressive resistance of helical piles subjected to seismic loads.

2 CONSIDERATIONS

The computation of the compressive resistance of helical piles subject to seismic loading is based on the following considerations:

(a) It is assumed that the helical piles are manufactured with multiple helices, spaced apart not more than 3 times the helix diameter.

(b) The helical pile compressive resistance comprises end bearing and CSR. The shaft friction is considered small and thus can be neglected.

(c) An incompressible soil plug will develop inside the helical pile.

(d) Shear waves do not produce volume changes or pore pressures in the soil during their propagation. However, the increase in pore pressure produced by the dilatational waves, which arrive first to the deep foundation location, is assumed to be still present once the shear waves arrive.

(e) The increase in soil shear stress (due to shear wave action and due to greater pile loads caused by the structure overturning moment) occurs at the same time the soil shear strength decreases (due to an increase in pore pressure).

(f) Soil is saturated.

(g) The soil layers are not susceptible to liquefaction.

(h) The soil index properties and mechanical and dynamic parameters have been determined in advance.

3 METHODOLOGY

3.1 General

The methodology to determine the compressive resistance of helical piles subjected to seismic loads requires analyzing the combined effects of an increase in soil shear stress (due to shear wave action plus greater pile loads due to the structure overturning moment) and a decrease in soil shear strength (due to an increase in pore pressure).

The methodology presented in the following sections is based on the research carried out by Zeevaert (1980, 1982, 1988 and 1991).

3.2 Increment in Pore Water Pressure Due to Dilatational Wave

The increment in pore water pressure due to dilatational waves has been studied by Zeevaert (1991), who developed a methodology based on the following rationale:

(a) The dilatational wave propagates from firm ground to the surface according to the following equation:

$$v_d{}^2 \frac{\delta^2 w}{\delta z^2} = \frac{\delta^2 w}{\delta t^2} \qquad [1]$$

where w is the vertical displacement and v_d is the dilatational wave velocity

(b) From theory of elasticity we know that the soil pressure σ_z is given by:

$$\sigma_z = E_c \frac{\delta w}{\delta z} \qquad [2]$$

where E_c is the dynamic soil modulus, given by :

$$E_c = 2(1+\nu)\mu \qquad [3]$$

where ν is the Poisson ratio and μ is the shear modulus, equal to :

$$\mu = v_d{}^2 \rho \frac{(1-2\nu)}{2(1-\nu)} \qquad [4]$$

where ρ is the unit mass of the soil, equal to the soil unit weight γ divided by the gravitational acceleration.

(c) Zeevaert (1991) solves Equation 2 as:

$$\sigma_z = -E_c w_o \frac{\pi}{2D} \sin\left(\frac{\pi}{2}\frac{z}{D}\right) \qquad [5]$$

where D is the depth between the ground surface and the firm ground, and w_o is the vertical displacement amplitude, given by :

$$w_o = \frac{4D^2}{\pi^2} \frac{\rho}{E_c} G_{av} \quad [6]$$

where G_{av} is the maximum vertical ground surface acceleration.

(d) Substituting Equations 3, 4 and 6 in 5 we obtain:

$$\sigma_z = -\left(\frac{2}{\pi} G_{av} D \rho\right) \sin\left(\frac{\pi}{2} \frac{z}{D}\right) \quad [7]$$

(e) During the earthquake, the increase in soil pressure in the saturated soil sediment occurs at constant volume, requiring the decrease in soil effective stress to be equal to the increase in pore water pressure, $\sigma_z = -u_z$, hence:

$$u_z = \left(\frac{2}{\pi} G_{av} D \rho\right) \sin\left(\frac{\pi}{2} \frac{z}{D}\right) \quad [8]$$

Equation 8 can be used to determine the increment in pore water pressure caused by the dilatational shear wave.

3.3 Decrease in End Bearing Resistance Due to Earthquake Loading

The increase in pore water will cause a decrease in effective stress and thus a decrease in end bearing. On this basis, when the helical pile end bearing resistance is computed, the pore water determined in Equation 12 should be subtracted from the vertical effective stress, which is then multiplied by the bearing factor Nq and helix area (assuming a pile tip plugged condition) to determine the pile end bearing resistance.

3.4 Increment in Soil Shear Stress due to Shear Wave

The shear waves propagate from the firm ground interphase into the soil deposits, producing important shear distortions in the soil mass. These distortions cause an increase in shear stress which is additive to the static shear stress acting on the soil prior to the earthquake (Figures 1 and 2). Furthermore, the shear waves are slower than the dilatational waves and hence arrive later at the place of observation. On this basis, it is considered that the pore pressure caused by the dilatational wave has already increased by the time the shear waves arrive at the foundation.

The increment in soil shear stress due to shear waves has been studied by Zeevaert (1980, 1982, 1988 and 1991), who presented the following methodology for the computation of the shear stress:

(a) The time required by the shear wave to travel through the full soil deposit, from firm ground to the surface, is equal to ¼ the soil dominant period T, therefore:

$$\frac{1}{4}T = \frac{D}{v_s} \quad [9]$$

where D is the depth between the ground surface and the firm ground, and v_s is the shear wave velocity. In stratified soil deposits, Equation 9 is modified as follows:

$$\frac{1}{4}T = \Sigma_{i=1}^{n} \frac{d_i}{(v_s)_i} \quad [10]$$

(b) The shear wave velocity is a function of the dynamic shear modulus μ as follows :

$$v_s{}^2 = \frac{\mu}{\rho} \quad [11]$$

(c) The dynamic shear modulus μ can be determined in the field from seismic cone penetration tests, cross-hole seismic surveys, downhole seismic surveys, or other field tests. Alternatively, it may be determined through laboratory tests in soil samples, which may include resonant column tests, free torsion pendulum tests, or other.

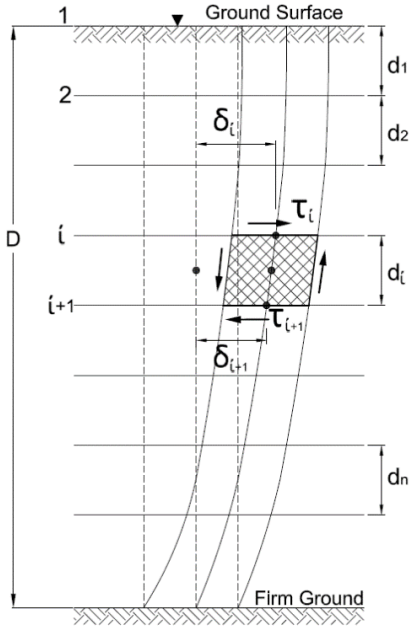

Figure 1. Shear stress due to shear wave.

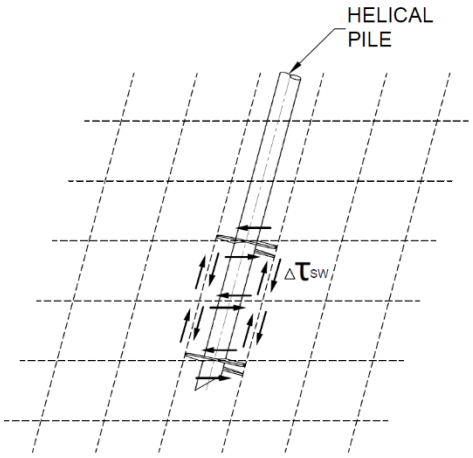

Figure 2. Shear stress on helical pile CSR due to shear wave

(d) The shear wave propagates from firm ground to the surface according to the following equation:

$$v_s{}^2 \frac{\delta^2 u}{\delta z^2} = \frac{\delta^2 u}{\delta t^2} \quad [12]$$

where u is the vertical displacement. Since the values of μ, ρ and consequently v_s change for every soil layer, Zeevaert (1982), developed an integration method to solve Equation 12 as follows:

(e) The algorithms for the computation of the maximum horizontal displacements δ_i and the corresponding shear stresses τ_i in each soil layer for the ground motion induced by the shear waves are given by:

$$\delta_{i+1} = A_i\, \delta_i - B_i\, \tau_i \quad [13]$$

$$\tau_{i+1} = C_i\, (\delta_i + \delta_{i+1}) + \tau_i \quad [14]$$

where the coefficients have the following values :

$$A_i = \frac{1 - N_i}{1 + N_i} \quad [15]$$

$$B_i = \frac{1}{1 + N_i} \left(\frac{\delta_i}{\mu_i}\right) \quad [16]$$

$$C_i = \frac{1}{2}\, \rho\, \delta_i\, \omega_n^2 \quad [17]$$

$$N_i = \frac{\rho\, \delta_i^2\, \omega_n^2}{4\mu_i} \quad [18]$$

and ω_n is the angular frequency of the soil mass, which initially can be computed from the soil period as follows:

$$\omega_n = \frac{2\pi}{T} \quad [19]$$

(f) The calculations start by computing a ground surface displacement δ_1 equal to :

$$\delta_1 = \frac{G_{av}}{\omega_n} \quad [20]$$

and assume that the increment in shear stress at the ground surface due to the shear wave is zero ($\tau_1 = 0$).

(g) Subsequently, Equations 13 and 14 are computed for each soil layer starting from the ground surface, using the coefficients in equations 15 to 18.

(h) When the calculations reach firm ground, the horizontal displacement computed should be zero. If this is not the case, the angular frequency initially assumed in Equation 19 should be corrected and a new iteration undertaken from the ground surface to the firm ground.

3.5 Increment in Soil Shear Stress due to Superstructure Overturning Moment Transferred to Piles

The rocking of the superstructure will increase the compressive loads acting on the piles. The increase in load may be determined from dynamic structural analyses, applying methods included in Building Codes.

An approach applicable when a rigid superstructure is supported on a rigid mat or box foundation supported by helical piles is shown in Figure 3. It is assumed that the underside of the foundation slab is not in contact with the soil underneath, therefore the vertical loads acting on the structure are directly transferred to the helical piles.

As a result of an earthquake, a horizontal seismic shear force V_M will be produced on a structure, acting on its center of mass located on a height h_M, producing a seismic overturning moment O_{TM} as shown in Figure 3. The overturning moment will produce dynamic loads on the piles, which will be additional to the static loads previously acting.

The procedure to determine the horizontal seismic shear force acting on the structure is included in Building Codes. The present Section does not summarize any procedure, rather it is assumed that the overturning moment has already been computed.

On this basis, the increase in pile load ΔP_i due to earthquake can be determined using the following equation:

$$\Delta P_i = \frac{M_y\, x}{\Sigma\, x^2} + \frac{M_x\, y}{\Sigma\, y^2} \qquad [21]$$

where M_y and M_x are the factored overturning moments due to earthquake loading and x and y are the distances of the piles to the center of gravity of the foundation. On this basis, the increase in the shear stress between the helices ΔCSR due to the increase in pile load ΔP_i due to earthquake is:

$$\Delta CSR = \frac{\Delta P_i}{\pi\,(D_h)\,(S_h)} \qquad [22]$$

where Dh is the helix diameter and Sh is the distance between the uppermost and lowermost helices.

3.6 Seismic CSR Resistance

The pile compressive resistance comprises shaft friction (often negligible), end bearing and CSR. The CSR applies to helical piles manufactured with multiple helices spaced not more than 3 times the helix diameter. The vertical displacement of a helical pile subjected to service conditions will typically be sufficient to develop full mobilization of shaft friction, partial mobilization of CSR, and small mobilization of end bearing, which requires relatively large displacements to fully develop. On this basis, a conservative assumption is that the CSR alone will have to resist the increase in pile load, which therefore requires the allowance of additional CSR resistance when helical piles in seismic regions are designed.

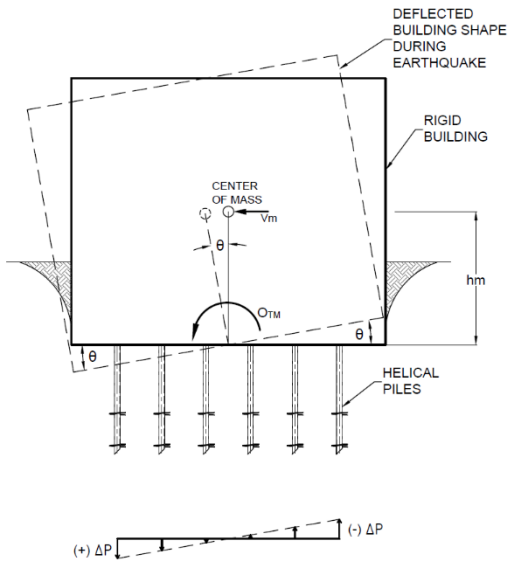

Figure 3. Pile loads due to overturning moment

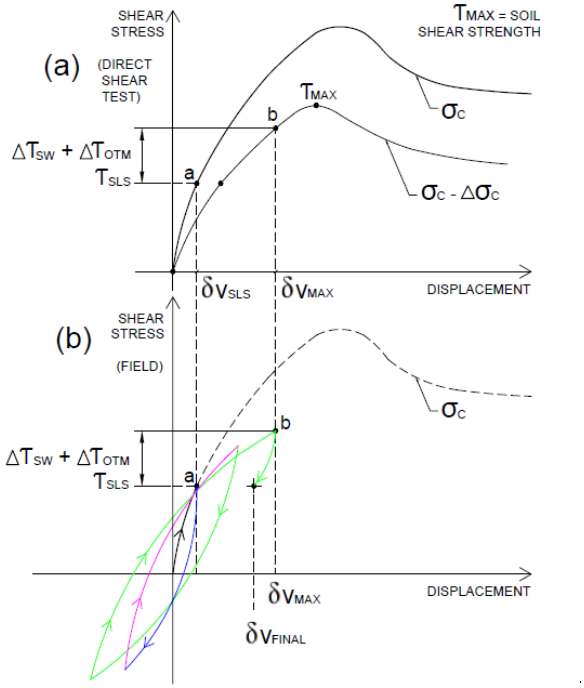

Figure 4. Shear stress increase acting on CSR

Once the decrease in soil shear strength and the increase in the soil shear stress due to earthquakes has been determined, the next step is to carry out laboratory tests to find out if the soil has adequate resistance to develop the necessary CSR to support the seismic loads. Triaxial cyclic tests or direct shear tests (cyclic or conventional) may be carried out. Direct shear tests are particularly desirable since the distortion produced in the soil sample during the test resembles the distortion of the soil between the helices when a helical pile is loaded in the field. The use of direct shear test results to understand the development of CSR under static loading has been applied by Padros (2013-1 and -2).

The shear stresses in the field and in a direct shear test are shown in Figure 4, where $\Delta\tau_{sw}$ is the additional soil shear stress due to the shear waves and $\Delta\tau_{OTM}$ is the additional soil shear stress due the increase in pile loads caused by the overturning moment acting on the superstructure. The confinement effective stress between the helices is σ_c. Furthermore, the dilatational wave produces an increase in pore pressure, which leads to a decrease in the confinement effective stress $\Delta\sigma_c$. Therefore, the direct shear test is carried out applying a compressive effective stress $\sigma_c - \Delta\sigma_c$. In that test, the total increase in shear stress due to sesimic loads is $\Delta\tau_{sw} + \Delta\tau_{OTM}$, which has to be compared with the maximum shear resistance of the soil.

4 EXAMPLE OF DETERMINATION OF COMPRESSIVE RESISTANCE OF HELICAL PILE SUBJECTED TO SEISMIC CONDITIONS

4.1 General

An example is presented to illustrate the computation of the compressive resistance of a helical pile subjected to seismic conditions. The example considers a rigid superstructure on a rigid shallow foundation supported by helical piles, as shown in Figure 5. The ULS and SLS static compressive loads on each pile are 30 ton and 21 ton, respectively. The overturning moments in the X and Y directions due to the horizontal seismic shear forces are 500 ton·m and 300 ton·m, respectively. A maximum vertical ground surface acceleration G_{av} of 1 m/sec^2 is considered. The subsurface conditions comprise granular and cohesive soil layers extending to 15.5 m depth, where firm ground is encountered. The groundwater level is located at the ground surface. The unit weight γ and the shear strength parameters (undrained shear resistance Cu and angle of internal friction φ) of each soil layer are presented in Table 1, which also includes the shear wave velocity determined from Seismic Cone Penetration Tests.

All helical piles have the same size, consisting of a 273 mm shaft diameter and two helices 762 mm diameter, located at 7.74 m and 9.26 m depth (helix spacing is 1.524 m). The piles' head is at 1 m depth, pinned to the slab. The piles' length is 8.6 m.

Table 1. Soil properties and parameters

Layer	z (m)	Soil Type	γ (ton/m^3)	Vs (m/s)	Cu (ton/m^2)	φ (deg)
A	0–4	Sand	1.80	110	0	28
B	4–6.5	Clay	1.85	40	25	0
C	6.5–10.5	Sand	1.90	105	0	30
D	10.5–13.0	Clay	1.85	60	25	0
E	13.0–15.5	Sand	1.90	100	0	32

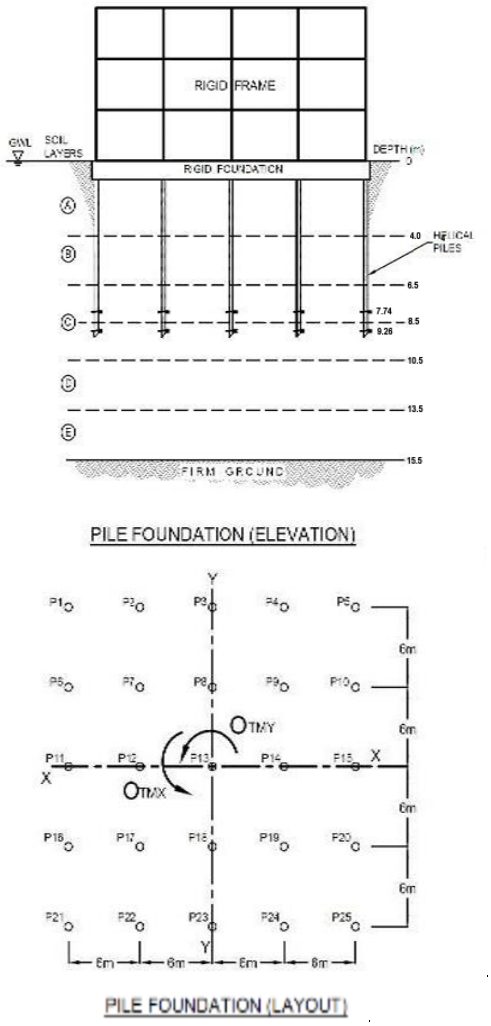

Figure 5. Building and soils conditions used in example

The unfactored compressive resistance Qc of the helical pile is 125 ton, comprising a Q_{CSR} of 18 ton, an end bearing Qeb of 107 ton and neglecting the shaft friction. Based on CFEM, applying a geotechnical resistance factor of 0.4 for deep foundations, the resulting factored compressive resistance ΦQc is 50 ton, adequate to support the ULS compressive load of 30 ton.

4.2 Considerations

The considerations included in Section 2 are applicable. Additional considerations comprise the following:

(a) Rigid superstructure on a rigid shallow foundation.

(b) The vertical loads acting on the structure are directly transferred to the helical piles (hence no contact between the underside of the rigid shallow foundation and the soil).

(c) The static SLS load acting on each pile is 21 ton. It is considered that a small vertical pile displacement is developed under service conditions, sufficient to fully mobilize the CSR. On this basis, the end bearing mobilized under SLS conditions is equal to 21 ton – 18 ton = 3 ton. It is noted that the size selected of the helical piles does not allow for additional CSR resistance in case of seismic loading.

(d) The vertical effective stress at mid-height between the helices (8.5 m depth) under static conditions is 7.1 ton/m^2 + 4.9 ton/m^2 = 12.0 ton/m^2, where 7.1 ton/m^2 is the vertical stress prior to pile installation and 4.9 ton/m^2 is the increase in vertical stress caused by the loaded pile under SLS conditions.

(e) The confining effective stress increases in the proximity of the pile after this has been installed. On this basis, the confining effective stress at mid-height between the helices under static conditions is considered equal to about 1.2 times the vertical effective stress (therefore equal to 8.7 ton/m^2).

(f) The shear stress acting in the soil on vertical planes between the helices under static pile loading conditions was calculated as (12 ton/m^2 – 8.7 ton/m^2)/2 = 1.65 ton/m^2

4.3 CSR Computation

(a) Initial calculations

The shear modulus and the ratios $\frac{d_i}{(v_s)_i}$ are presented in Table 2. From that Table and Equations 10, 19 and 20 we obtain the soil period T = 0.82 sec, angular frequency ω_n = 7.7 sec^{-1} and ground surface displacement δ_1 = 0.017 m.

Table 2. Soil mass, shear modulus and $d_i/(Vs)_i$ ratios

Layer	d_i (m)	ρ (ton·sec^2/m^4)	μ (ton/m^2)	$d_i/(Vs)_i$ (sec)
A	4	0.184	2,225	0.036
B	2.5	0.189	300	0.063
C	4	0.194	2,140	0.038
D	2.5	0.189	680	0.042
E	2.5	0.194	1,940	0.025

(b) Increment in pore pressure caused by dilatational wave

The increment in pore water pressure is computed from Equation 8, considering an average unit mass of the soil ρ equal to 0.190 ton·sec/m^4. Substituting the parameters in Equation 8, we obtain the increment in pore water pressure caused by the dilatational wave, using the equation below. The results are summarized in Table 3.

$$u_z = [\frac{2}{\pi}\left(1\ \frac{m}{sec^2}\right)\ 15.5\ m\ (0.190\ \frac{ton\cdot sec^2}{m^4}\ ]\sin\left(\frac{\pi}{2}\ \frac{z}{15.5\ m}\right)$$

$$u_z = 1.87\sin(\frac{\pi\ z}{31})$$

Table 3. Increment of pore water pressure due to dilatational waves

z (m)	Uz (ton/m^2)	z (m)	Uz (ton/m^2)	z (m)	Uz (ton/m^2)
0	0	8	1.36	12	1.75
2	0.38	8.5	1.42	14	1.85
4	0.74	9.3	1.51	15.5	1.87
6	1.07	10	1.59		

(c) Increment in soil shear stress due to shear wave

From Equation 20 the ground surface displacement δ_1 = 0.017 m is obtained. In accordance with the method hypothesis, the increment in shear stress at the ground surface due to the shear wave is zero ($\tau_1 = 0$). Subsequently, Equations 13 and 14 are computed for each soil layer starting from the ground surface, using the coefficients in Equations 15 to 18. The results are included in Table 4. The computation results indicate that the horizontal displacement computed at firm ground is zero, which indicates that the angular frequency initially assumed in Equation 19 is correct, and there is no need to carry out another iteration.

(d) Increment In soil shear stress due to overturning moment transferred to piles

The increase in pile load ΔP_i due to earthquake condition is computed using Equation 21, considering $\Sigma x^2 = \Sigma y^2 =$ 1,800 m^2. The maximum increase will occur in two corner piles (designated No's. 5 and 21 in Figure 5), obtaining ΔP_i = ± 5.3 ton in each of them.

Consequently, the increase in the shear stress between the helices due to the increase in pile load ΔP_i due to earthquake is:

$$\Delta CSR = \frac{\Delta P_i}{\pi\ (D_h)\ (2\ D_h)} = \frac{5.3\ ton}{\pi\ (0.762\ m)\ (2\cdot 0.762\ m)}$$

$$\Delta CSR = 1.45\ \frac{ton}{m^2}$$

(e) Computation of total CSR increase

The total increase in shear stress acting on vertical planes between the helices ΔCSR_{TOTAL} comprises the increase in shear stress due to shear wave action and due to greater

pile loads caused by the structure overturning moment, therefore:

$$\Delta CSR_{TOTAL} = 1.27\ \frac{ton}{m^2} + 1.45\ \frac{ton}{m^2} = 2.72\ \frac{ton}{m^2}$$

As mentioned in Section 4.2 consideration (f), the initial shear stress acting on the soil under static conditions (on vertical planes between the helices) is 1.65 ton/m^2. Therefore, the total CSR adding the static plus the dynamic increment is:

$$CSR_{TOTAL} = 1.65\ \frac{ton}{m^2} + 2.72\ \frac{ton}{m^2} = 4.37\ \frac{ton}{m^2}$$

In order to determine the effect that the increase in pore pressure has in the shear resistance, direct shear tests can be carried out in representative soil samples retrieved from the soil layers where the helices will be located. In the present example, the results from direct shear tests undertaken in a sample obtained from layer C are shown in Figure 6. The figure shows that compressive stress of 8.7 ton/m^2 resulted in a shear strength of 5 ton/m^2, corresponding to Φ = 30 degrees. The results of a second direct shear test where the increase in pore pressure was deducted from the compressive stress are also shown (i.e, 8.7 ton/m^2 – 1.42 ton/m^2 = 7.28 ton/m^2), which resulted in a shear strength of 4.2 ton/m^2, for the same Φ = 30 degrees. It is noted that the CSR exceeds the shear strength under earthquake loading (4.37 ton/m^2 > 4.2 ton/m^2) which means that the pile will have to rely on end bearing to support the earthquake compressive load.

$$Q_{CSR_{SIS}} = 4.2\ \frac{ton}{m^2}\ \pi\ (0.762\ m)\ (2\ \cdot\ 0.762\ m)$$

$$Q_{CSR_{SIS}} = 15.3\ ton$$

Note that 15.3 ton < 18 ton. As an alternative to increase Q_{CSR} and Q_{CSRSIS}, the helix spacing could be increased to 2.5Dh or 3 Dh, or a third helix could be added.

Table 4. Computation of increment of soil shear stress and displacements due to shear wave

Depth (m)	Layer	d_i (m)	ρ (ton·sec^2/m^4)	μ (ton/m^2)	N_i x10^{-3}	A_i	B_i x10^{-3}	C_i (ton/m^3)	δ_i (m)	τ_i (ton/m^2)
0									0.017	0
	A	4	0.184	2,225	19.6	0.96	1.76	21.82		
4									0.016	0.73
	B	2.5	0.189	300	58.4	0.89	7.87	14.01		
6.5									0.009	1.08
	C	4	0.194	2,140	53.7	0.99	0.93	11.50		
10.5									0.006	1.43
	D	2.5	0.189	680	25.8	0.95	0.35	14.01		
13									0.001	1.54
	E	2.5	0.194	1,940	9.3	0.98	1.28	14.38		
15.5									0.000	1.54

(f) Computation of Seismic End Bearing

The seismic end bearing Qeb_{SIS} is computed by deducting the increment in pore pressure as follows:

$$Qeb_{SIS} = Nq(\sigma_z - u_z)Ah \qquad [24]$$

where σ_Z = 7.81 ton/m^2 at 9.3 m depth. From Table 3, Uz = 1.51 ton/m^2. Nq is the bearing factor, equal to 30 (Zeevaert 1982) for Φ = 30 degrees. Furthermore, the helix area Ah is determined for a helix diameter of 762 mm, assuming a pile tip plugged condition. Equation 24 results in Qeb_{SIS} = 86.2 ton, which is about 20% smaller than the static 107 ton.

(g) Compressive Resistance of Helical Pile Subjected to Seismic Load

The seismic compressive resistance is determined by adding the seismic CSR and end bearing, as follows:

$$Q_{C_{SIS}} = 15.3\ ton + 86.2\ ton = 101.5\ ton$$

$$\Phi Q_{C_{SIS}} = 40.6\ ton\ > 30\ ton$$

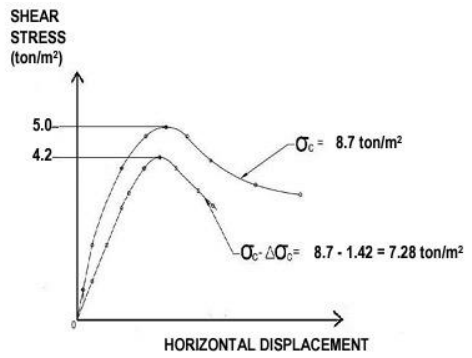

Figure 6. Shear stress computation based on the results of a direct shear test.

5 CONCLUSIONS

1. The determination of the compressive resistance of helical piles subjected to seismic loads requires assessing the effects that dilatational waves and shear waves produce in a saturated soil mass.

2. Increases in shear stress result from the propagation of seismic shear waves and due to the increase in pile loads caused by superstructure overturning moments. Additionally, the dilatational wave produces an increase in pore pressure, causing a decrease in the effective stress and consequently a decrease in the soil shear strength.

3. The increase in shear stress due to the shear wave and the decrease in shear strength due to the dilatational wave can be determined by applying Zeevaert's theory. The methodology to determine the increase in pile loads caused by the seismic overturning moment can be found in Building Codes.

4. The CSR_{SIS} resulting from the increase in shear stress due to the shear wave in combination with the reduction in shear strength due to the increase in pore pressure can easily be smaller than the soil shear strength acting on vertical planes between the helices of the loaded pile, resulting in a greater load transferred to the lowermost helix, increasing the demand for end bearing resistance, which simultaneously is reduced due to the increase in pore pressure.

5. Alternatives to increase the CSR_{SIS} include extending the helix spacing up to 3 Dh or installing more helices.

6. An example is included to illustrate the application of the method.

ACKNOWLEDGEMENT

The authors are grateful to Hector Ibarra, P. Eng. with Almita Piling Inc. for his help preparing the figures.

REFERENCES

Padros, G. (2013). Analysis of Cylindrical Shear Resistance of Screw Piles Subjected to Compressive Loads Based on Direct Shear Tests. *1st International Symposium on Helical Piles*. Amherst, Massachusetts.

Padros, G. and Schmidt, R. (2018). Performance of Helical Pile Cylindrical Shear Resistance in Earthquake Loading. *12th Canadian Conference on Earthquake Engineering.* Quebec, QC.

Padros, G. and Schmidt, R. (2019). Cylindrical Shear Resistance of Helical Piles Subjected to Seismic Loads. *Canadian Geotechnical Conference*, St. John's, Newfoundland.

Zeevaert, Leonardo (1980). *Interaccion Suelo – Estructura de Cimentacion.* Editorial Limusa. Mexico.

Zeevaert, Leonardo (1982). *Foundation Engineering for Difficult Subsoil Conditions*. Second Edition. Van Nostrand Reinhold, New York.

Zeevaert, Leonardo (1988). *Seismo-Geodynamics of the Ground Surface*. Editora e Impresora Internacional, S.A de C.V., Mexico.

Zeevaert, Leonardo (1991). "Foundation Problems in Earthquake Regions". *Foundation Engineering Handbook.* Fang, H.Y. (Editor). Second Edition. Chapman & Hall, New York.